Numerical Tools for Fracture of MEMS Devices

N. Tayebi*, A. K. Tayebi**, and Y. Belkacemi***
*Department of Mechanical and Aerospace Engineering, Case Western Reserve University
**Department of Civil Engineering, Cornell University
***Ecole Nationale Polytechnique of Algeria
nxt23@po.cwru.edu, akt1@cornell.edu

Abstract

Numerical tools to model fracture in MEMS devices are proposed. The two numerical procedures are the Element Free Galerkin method and the Displacement Discontinuity Method. Experiments on MEMS fracture are used to evaluate the numerical procedures. The test specimens covered a range of geometries and designs, including notches, holes and corners. For some specimens both methods gave acceptable results compared to experiments (Ballarini et al and Suwito), while for others results were off by more than 15%. These findings raise new questions about the applicability of linear elastic fracture mechanics to model failure of MEMS devices at microscopic scale.

Key words: CAD Tools, MEMS, Fracture Mechanics, Meshless Methods, Boundary Element Methods.

1. Introduction

MEMS are commonly made of Silicon whose mechanical properties are relatively well known at macroscale but still under investigation at microscale. Behavior at microscale can be fundamentally different than at macroscale requiring from the MEMS community to establish, and with high reliability, the mechanical properties of MEMS materials and standard tests to determine these properties. While there is a wealth of ASTM standard tests for the determination of mechanical properties, almost none of them can be implemented (as is) at microscale because of the impossibility of similar instrumentation at microscale. As such, new numerical tools and test procedures need to be developed and be proved reliable. From a mechanical perspective, elastic constants, the complete stress-strain curve, and the fracture and fatigue properties at temperatures and environments similar to those where MEMS operate need to be determined in order to achieve efficient design and reliable products. Since MEMS are made of either single crystal silicon or polysilicon, these mechanical properties need to be determined for each crystal facet ({100}, {111}) and for polysilicon.

This paper investigates the application of numerical fracture modeling to simulate experiments. The numerical procedures are the element free Galerkin meshless method and a variant of the boundary element method called the displacement discontinuity method. The applicability of these two methods at MEMS scale gives acceptable results compared to experiments, which can lead us to answer to some questions like: Is linear elastic fracture mechanics (LEFM) applicable for MEMS fracture? Are size effects important? Do flaws, corners, notches, and holes enhance the fracture mechanical properties of MEMS devices?

The mathematical foundation of the numerical methods is presented first and followed by simulation of experiments.

2. The displacement discontinuity method

The displacement discontinuity method (DDM) is based on the analytical solution for a constant displacement discontinuity on several straight segments within an infinite elastic region. It consists in dividing one of these segments into N elements linked to each other, and in considering the displacement discontinuity to be constant over each one. Thus, by knowing the analytical solution for each constant elemental displacement discontinuity, we sum the effects for all N elements to find the numerical solution. It is also a means of finding a discrete approximation to the smooth distribution of relative displacement (i.e displacement discontinuity) that exists in reality. Each segment is a boundary element and represents an elemental displacement discontinuity defined in the s , n directions as shown in Figure 1, and its components D_s and D_n
are defined as follow :

$$D_s = u_{s^-} - u_{s^+}$$
$$D_n = u_{n^-} - u_{n^+} \quad (1)$$

where u_s *and* u_n are the radial and tangential displacements.

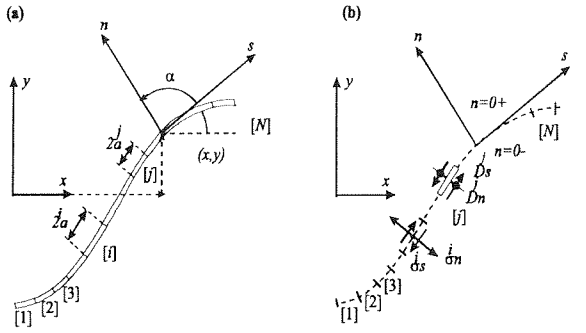

Figure1: Representation of a crack by N elemental displacement discontinuities.

The effects of a single displacement discontinuity on the displacements and stresses at an arbitrary point in the infinite plate can be computed. In particular, the radial and tangential stresses at the midpoint of the ith element can be expressed in terms of the displacement discontinuity components at the jth element as follows:

$$\begin{cases} \sigma_s^i = A_{ss}^{ij} D_s^j + A_{sn}^{ij} D_n^j \\ \sigma_n^i = A_{ns}^{ij} D_s^j + A_{nn}^{ij} D_n^j \end{cases} \qquad i = 1,N \quad (2)$$

Where A_{ss}^{ij} . . . etc, are the boundary influence coefficients for the stresses. The coefficient A_{sn}^{ij}, for example, gives the radial stress at the midpoint of the ith element due to a constant unit tangential displacement discontinuity ($D_n^j = 1$) over the jth element.

If we specify the values of the radial and tangential stresses σ_n^i and σ_s^i for each element, we will have a system of 2N linear equations in 2N unknowns, namely the elemental displacement discontinuity components D_s^i and D_n^i.

After solving the above equations, we can find the displacements and stresses at designated points in the studied body by using the same principle. The implementation of Fracture mechanics consists in the determination of the strain energy release rate G. G is compute in terms of strain and stress on the boundaries of the cracked region. Considering the problem to be 2D and the material to be linear elastic. The surface forces T_i, are imposed on the boundary of the cracked region Ω_T and the displacements u_I are imposed on the remaining part Ω_U.

$$G = \frac{1}{2}\int_{\Omega}\left(T_i \frac{du_i}{dA} + u_i \frac{dT_i}{dA}\right) d\Gamma \quad (3)$$

The previous expression allows the computation of G knowing the displacements and stresses on the outer contours. In our applications, Ω_U will not exist generally (Ω_U =0). The DDM allows the determination of the stresses and displacements on the boundary and in every point of the structure.

When stresses are applied, Equation 3 can be written as:

$$G = \frac{1}{2}\int T_i \frac{du_i}{dl} d\Gamma \quad (4.a)$$

This expression is written in an incremental form, where the displacements before and after crack growth of length *dl are* designated by u_i^1 et u_i^2. The term inside the integral expression is written as:

$$T_i\, du_i = T_i\left(u_i^2 - u_i^1\right) \quad (4.b)$$

then equation 4 is written as:

$$G\, dl = \int_{\Omega} T_i\left(u_i^2 - u_i^1\right) d\Gamma + \int_{\Gamma} T_i\left(D_i^2 - D_i^1\right) d\Gamma \quad (5)$$

Thus, the numerical computation of G is done by the discretization of Equation (5). We obtain a sum of the products $T_i\left(u_i^2 - u_i^1\right)$ on the contour Ω and of the products $T_i\left(D_i^2 - D_i^1\right)$on the crack.

3. The element free Galerkin Method

The element free Galerkin method (EFGM) is a meshless method and is suitable for problems with changing geometry such as crack propagation since it does not require any meshing. The crack is simply considered as a boundary extension. The numerical procedure is quite similar to that of finite element except that, in EFGM, least square interpolants are used to approximate the dependant variables. These interpolants use an influence domain to define the connectivity between nodes.

For an arbitrary point $x \in \Omega$, we define a small domain Ω_x surounding this point with $\Omega_x \subset \Omega$. Considering a function $u(x)$ where x=(*x, y*) defined on the domain Ω. Thus for any given point $x \in \Omega_x$, the function $u(x)$ is approximated by :

$$u(x) = \sum_j^m p_j(x)\, a_j(x) = p^T(x)\, a(x) \quad (6)$$

where $p_j(x)$ are monomials in the space coordinates $x^T = [x, y]$ and $a_j(x)$ are coefficients that are function of x. a(x) are obtained by using the L-norm which consists in minimizing the expression:

$$J = \sum_{I}^{n} w(x - x_i)\left[p^T(x_I)a(x) - u_I\right]^2 \quad (7)$$

where n is the number of points in the neighborhood of x where the weight function $w(x - x_I) \neq 0$, and u_I is the nodal value of u for $x = x_I$. Equation (7) leads to the following linear relations between a (x) et u_I :

$$A(x)\, a(x) = B(x)\, u \quad (8)$$

where A(x) and B(x) are defined as :

$$A(x) = \sum_{I}^{n} w_I(x)\, p^T(x_I)\, p(x_I) \quad (9)$$

$$B(x) = \left[w_1(x)p(x_1),\, w_2(x)\, p(x_2),\ldots,\, w_n(x)\, p(x_n)\right] \quad (10)$$

by defining the shape functions as :

$$\phi_I(x) = \sum_{j}^{m} p_j(x)\,(A^{-1}B(x))_{jI} \quad (11)$$

$u^h(x)$ can be writen as :

$$u^h(x) = \sum_{I}^{n} \phi_I(x)\, u_I \quad (12)$$

In this work, the exponential weight function is selected and is defined as:

$$w_I\left(d_I^{2k}\right) = \begin{cases} \dfrac{e^{-(d_I/c)^{2k}} - e^{-(d_{mI}/c)^{2k}}}{\left(1 - e^{-(d_{mI}/c)^{2k}}\right)}, & d_I \le d_{mI} \\ 0, & d_I > d_{mI} \end{cases} \quad (13)$$

Finally, the problem is solved by a stiffeness equation Ku = f where K and f are composed of submatrices K_{IJ} (2×2) and f_I (2×1) given by:

$$K_{IJ} = \int_{\Omega} B_I^T D B_J \, d\Omega - \int_{\Gamma_u} \phi_I \, SNDB_J \, d\Gamma - \int_{\Gamma_u} B_I^T D^T N^T S \phi_J \, d\Gamma \quad (14)$$

and

$$f_I = \int_{\Gamma_t} \phi_I \, \bar{t} \, \delta d\Gamma - \int_{\Omega} \phi_I b \delta d\Omega - \int_{\Gamma_u} B_I^T D^T N^T S \bar{u} \, d\Gamma \quad (15)$$

where D is the elastic matrix and

$$B_I = \begin{bmatrix} \phi_{I,x} & 0 \\ 0 & \phi_{I,y} \\ \phi_{I,y} & \phi_{I,x} \end{bmatrix} \quad (16)$$

$$N = \begin{bmatrix} n_x & 0 & n_x \\ 0 & n_x & n_x \end{bmatrix} \quad (17)$$

$$S = \begin{bmatrix} s_x & 0 \\ 0 & s_y \end{bmatrix} \quad (18)$$

$$s_{x,y} = \begin{cases} 1 \text{ if } u_{x,y} \text{ is prescribed on } \Gamma_u \\ 0 \text{ if } u_{y,x} \text{ is prescribed on } \Gamma_u \end{cases} \quad (19)$$

Fracture mechanics concepts are introduced by defining the domain of the J integral near the crack tip.

4. Application to MEMS fracture

The two methods were used to simulate experiments conducted by Ballarini et al (1997) and Suwito and Dunn.

Case study 1

The test setup of Ballarini et al (1997) is shown in fig.2 and the numerical model in fig.3. The length x which corresponds to the uncracked ligament has three values 6, 10 and 20μm . A probe was used to open the notch (the notch is considered as sharp crack in the mathematical model) to cause fracture where the prescribed displacement u=4μm corresponds to the probe wedge. Polycrystalline silicon was considered isotropic with a Young's modulus and a Poisson's ratio respectively equal to 160 GPa and 0.22. In this example, we considered the same assumptions as Ballarini et al.

For the DDM, 300 elements were considered out of which 150 were used for the crack discretization. For the EFGM, 600 uniformly distributed nodes were used. Figures 4.(a) and (b) show the variation of the stress intensity factor in terms of the distance of the probe tip from the crack tip. Both methods gave perfectly concordant results with those obtained by Ballarini et al.

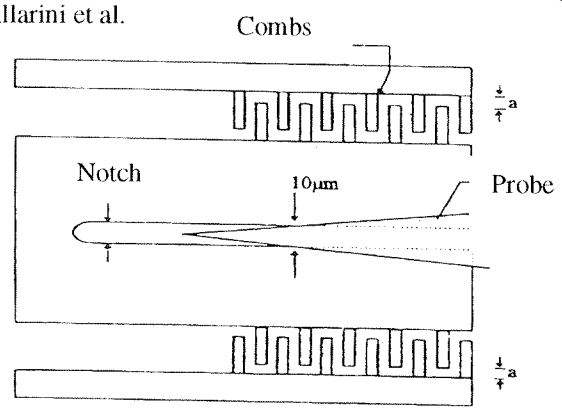

Figure 2: Schematic of the Test setup

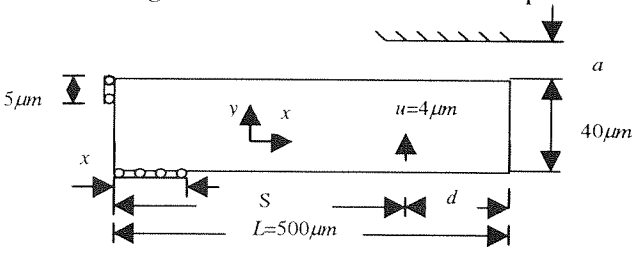

Figure 3 : Half of the mathematical model

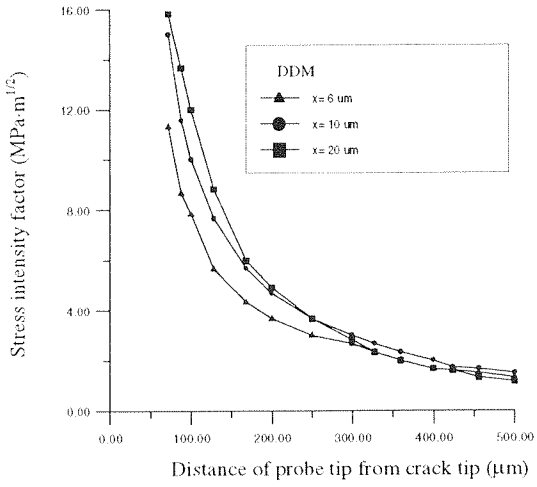

(a)

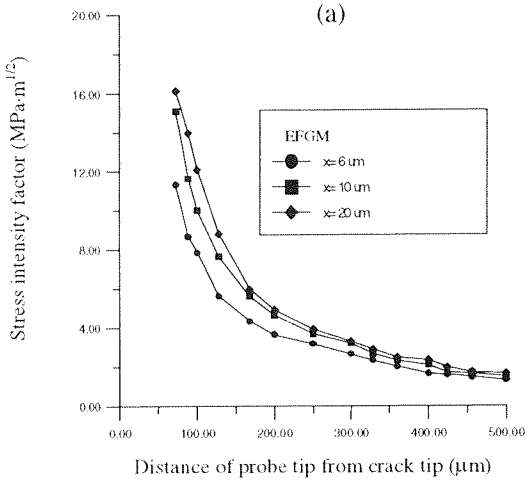

(b)

Figure 4: Stress intensity factor vs. probe position for comb distance equal to infinity, (a): DDM, (b): EFGM.

Case study 2

Suwito and Dunn (1997) studied the effect of notch depth on a 3-point beam made of single crystal silicon. They considered silicon to be anisotropic, as such only EFGM was used, since our DDM formulation was based on isotropic assumptions.

The specimen is shown in Fig. 5. The dimensions of the specimen are L = 20 mm, b=1.5 mm, h=1.08 mm and a was equal to either 0.093mm, 0.147 mm, 0.164 mm or 0.210 mm. For this example, 800 uniformly distributed nodes were used. Results obtained by using EFGM are compared to those obtained by Suwito and Dunn in Table 1.

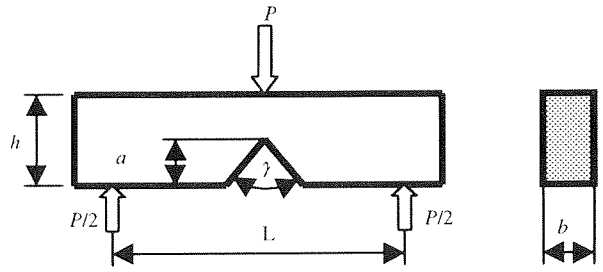

Figure 5: 3 point flexure beam used by Suwito (notch angle = 70.53°).

Table 1: Stress intensity factor of 70.53° notched beams with four different notch depths.

	K_I (MPa·m$^{0.5}$)	
	a=0.093mm σ_r =86.19 MPa	a=0.147mm σ_r =61.90 MPa
Suwito	0.81	0.73
EFGM	0.68	0.69
	K_I (MPa·m$^{0.5}$)	
	a=0.164mm σ_r =61.15 MPa	a=0.210mm σ_r =52.60 MPa
Suwito	0.76	0.74
EFGM	0.65	0.67

5. Conclusion

Non-conventional boundary element and finite element methods were successfully used, with different degrees of success, for the simulation of silicon MEMS fracture experiments with the assumption of the applicability of linear elastic fracture mechanics (LEFM). Further simulations need to be carried before assessing the reliability of these methods.

References

[1] Crouch, S. L and Starfield, A. M., "Boundary element method in solid mechanics". Allen and Unwin (1983).

[2] Belytschko, T., Gu, L., and Lu, Y.Y., "Fracture and Crack Growth by Element-Free Galerkin Methods'', Journal of Mater. Sci. Eng, 1995, pp. 519-534.

[3] Ballarini, R., Mullen, R.L., Yin, Y., Kahn, H., Stemmer, S., and Heuer, A.H., "The Fracture Toughness of Polysilicon microdevices", J. Master. Res, Vol.12, N° 4, Apr 1997, pp. 915-922.

[4] Suwito, W., "Fracture of Notched Silicon Microstructures", PhD Dissertation, University of Colorado at Boulder, 1997.

[5] Tayebi, N., "Etude du phenomene de rupture des structures MEMS", Ingenieur d'Etat Thesis, Ecole Nationale Polytechnique.